JOURNAL OF THE HYDRAULICS DIVISION

Scour Around Bridge Piers at High Flow Velocities

By Subhash C. Jain,[1] M. ASCE and Edward E. Fischer,[2] A. M. ASCE

Introduction

Scour around bridge piers has been the subject of many investigations (1,2,3,4,6,8,11), throughout the world, and numerous scour prediction formulas have been published as results of these studies. But predicted scour depths vary widely, especially when the formulas are applied to flow conditions outside the range of conditions for which they were developed. However, in spite of the variations, there does appear to be a consensus. Once the conditions of general sediment motion have been established in a stream, there will be no further increase in scour depth with velocity, because the rate at which sediment enters the region of scour is equal to the rate of removal by the scouring process. As a result, few investigations have been made for flows at higher velocities, i.e., for flow regimes well beyond the onset of general sediment transport.

The mechanism of local scour is well understood. In summary, when an obstruction such as a blunt-nosed pier is placed in a flow field, locally higher velocities are produced around the pier which increase the tractive force on the sediment at the pier base. Also, due to the nonuniform velocity distribution in a streamflow, the pressure field induced by the pier: (1) Creates a downward velocity along the lower leading face of the pier; and (2) produces a three-dimensional separation of the boundary layer leading to the formation of a horseshoe vortex. According to Melville (6), once the process has begun, it is the downward flow impinging on the bed, and the horseshoe vortex transporting dislodged particles away, which form the dominant scour mechanism. In the case of clear water scour (i.e., pier scour in a stream in which there is no net sediment transport other than wash load), as the scour depth increases, the strength of the downflow decreases near the bottom until finally, it can no longer dislodge

Note.—Discussion open until April 1, 1981. To extend the closing date one month, a written request must be filed with the Manager of Technical and Professional Publications, ASCE. This paper is part of the copyrighted Journal of the Hydraulics Division, Proceedings of the American Society of Civil Engineers, Vol. 106, No. HY11, November 1980. Manuscript was submitted for review for possible publication on August 30, 1979.

[1]Assoc. Prof. and Research Engr., Energy Div., Inst. of Hydr. Research, Univ. of Iowa, Iowa City, Iowa.

[2]Grad. Student, Inst. of Hydr. Research, Univ. of Iowa, Iowa City, Iowa.

particles. This condition represents the maximum scour to be attained by the prevailing flow conditions. Experimental observations show that the side slopes of the scour hole in the clear water regime are approximately equal to the natural angle of repose of the bed material. This indicates that the scour mechanism is in the immediate vicinity of the pier base, and that sediment slides in toward the base before it is removed. In the case in which there is a net sediment transport in the stream, the strength of the downflow near the bottom similarly decreases with increasing scour depth, but maximum scour is attained when the rate of sediment removal is equal to the rate of sediment transported into the scour hole by the stream. The visual observation of the scour process in the sediment transport regime at high flow velocities, as described later, shows that a dynamic equilibrium exists between scour hole and streamflow which is not apparent when the flow is stopped; the flow field near the base of the pier is strong enough to support the sides of the scour hole at angles greater than the angle of repose of the sediment. The wall periodically collapses and dumps sediment into the hole, either as a dune encroaches upon the pier, or

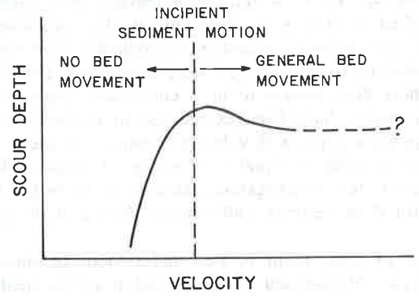

FIG. 1.—Scour Depth Versus Flow Velocity

as the fluid forces supporting it become unstable. The maximum scour depth under such unstable conditions cannot be accurately measured either by observation or after stopping the flow.

In terms of stream velocity, maximum scour depth around a pier increases with increasing velocity until incipient sediment movement conditions in the stream are reached (see Fig. 1). Experimental observations (3,11), then show that as the stream velocity is further increased, scour depth no longer increases but, in fact, decreases slightly, because there is now also a sediment discharge into the scour hole. Still further increases in stream velocity have shown that the maximum scour depth no longer increases (3). This last observation has not been seriously challenged in the literature, because most work has been concerned with predicting maximum scour, which is believed to occur as clear water scour.

The object of the present study, therefore, was to investigate the effect of flows at high velocities on scour depths around piers. Scour experiments were conducted on solitary circular piers in which pier size, mean sediment size,

and velocity were systematically varied. A special technique was used to measure the maximum scour depths. It was observed that scour depth does increase at higher velocities, contrary to the previously mentioned consensus. During the experiments, an attempt at scour visualization was made by placing half-piers against the flume wall.

Experimental Setup and Procedures

Flume.—The experiments were conducted in a glass-walled tilting sediment flume of the Iowa Institute of Hydraulic Research. The working section of the

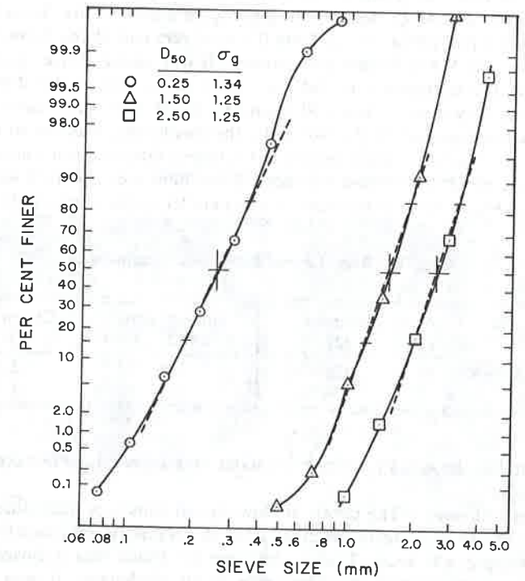

FIG. 2.—Size Frequency Graph for Three Sands

flume was 27 m long, 91 cm wide, and 45 cm deep. Water and sediment were recirculated by two axial-flow, variable-speed pumps, each pump discharging into its own 20-cm return line. Flume discharge was measured by a calibrated orifice meter in each line; the combined maximum discharge was 160 L/s. Piezometers for measuring local water surface elevations were located in the floor of the flume at 3.05-m intervals. The piezometers were connected to a central manometer board to facilitate the determination of the slope of the water surface. The slope of the flume could be changed while it was operating by means of an electrically driven tilting mechanism. A pair of 2.54-cm diameter rails supported by the flume walls served as the vertical reference for all elevation

measurements. A motorized instrument carriage rode on the flume rails along the full length of the channel. A standard point gage with a vertical resolution of 0.03 cm was used to measure elevations.

Bed Material.—Three sizes of sand were used as bed material. The fine sand was laboratory grade white quartz, and the medium and coarse sands were locally obtained filter sands. Sieve analyses were conducted after recommendations by Vanoni, et al. (13). Fig. 2 is a plot of the analysis and results, and Table 1 is a summary of the sediment characteristics. The variables D_{50} and σ_g, are the mean sediment size and the geometric distribution of sediment diameters about the mean, respectively.

Piers.—The piers were made from clear plastic pipes, 5.08 cm and 10.16 cm in diameter, and 43 cm long. Both piers were placed in the flume for each run, the leading pier about 10.5 m from the upstream end of the flume channel, and the other pier 9.2 m further downstream. It was assumed that disturbances produced by the upstream pier did not affect scour around the downstream pier, because they were at least 90 diameters apart where the mean velocity distribution is self-preserved (5). Normally, the smaller pier was placed upstream from the larger one, but in a few tests with the largest discharges, it was necessary to reverse the order. This was done because the flume would not tilt sufficiently for the equilibrium flow to establish a bed parallel to the flume rails, and the downstream bed degraded too much for scour measurements to be taken around the larger pier.

TABLE 1.—Bed Material Sizes and Distributions

Variable (1)	Fine sand (2)	Medium sand (3)	Coarse sand (4)
D_{50}, in millimeters	0.25	1.50	2.50
σ_g	1.34	1.25	1.25

Flow Establishment.—The depth of flow for all runs was maintained at 10.2 cm, except for the depth tests described later. A volumetric approach to maintain a constant depth was used. That is, because the flume was a closed system, the volume of water in it was the same at all discharges. It was observed that the average bed elevation did not change from run to run.

Uniform flow conditions were established with the piers in place for each run, by setting the discharge and then adjusting the slope of the flume until the bed and water surface slopes were nearly parallel to each other. Once uniform flow was established, the flow was stopped, the flume drained, and the bed around each pier prepared for measuring scour (as described later). The flume was then filled again and the run made under the established uniform flow conditions. Experiments in which dunes were present, were allowed to run long enough for several sand dunes to pass the piers; otherwise, the experiment was run until it was determined that approximate maximum scour was reached, generally determined by observation of the scour process from within the pier.

The water surface slope for each run was determined from the piezometer readings obtained from the manometer board. At the greater discharges where

the readings fluctuated widely, the minimum and maximum values at each station were averaged to obtain values for computing the slope. A linear regression program was used to determine the best-fit line to the water surface slope data for each run.

After each scour run, the bed profile along the center line of the flume was measured with a sonic sounder. A linear regression analysis was performed on the data to determine the bed slope and the mean bed elevation (MBE) at each pier.

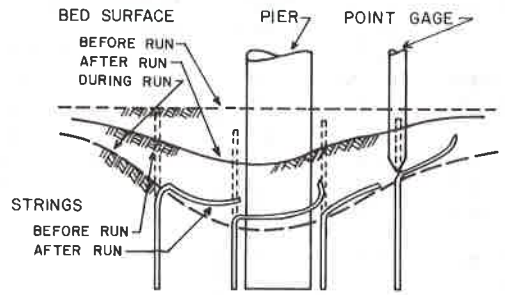

FIG. 3.—Schematic of Scour Measurement Method

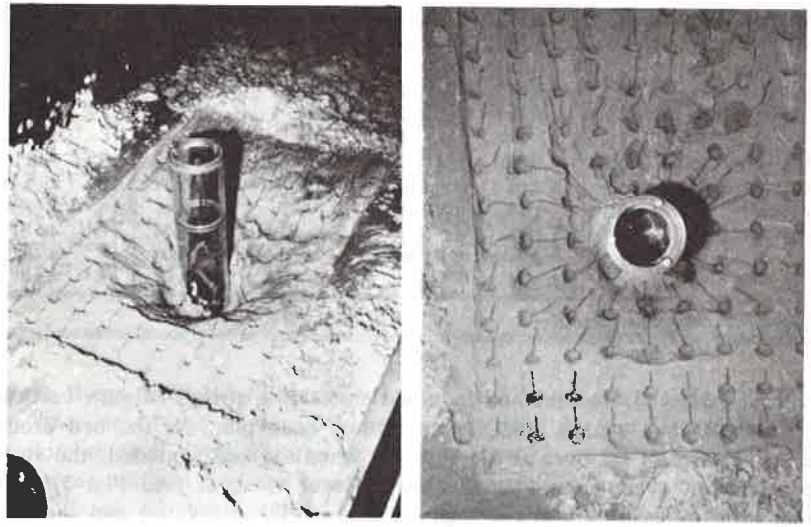

FIG. 4.—Photographs of String Grid and Excavation Work

Scour Measurement.—During the initial phases of the project, it became apparent that the maximum scour depth was not reflected accurately by the conditions around the piers after a run, because the scour holes were partially filled in as the flow was stopped. Borrowing an idea from Miller and Leopold (7), who used chains to measure scour in the field, a means of recording maximum

TABLE 2.—Summary of Test

Run number (1)	Sediment size, D_{50}, in millimeters (2)	Flow depth, y_o, in centimeters (3)	Mean velocity, U_o, in meters per second (4)	Froude number, $F = U_o/\sqrt{gy_o}$ (5)	Critical Froude number, $F_c = U_c/\sqrt{gy_o}$ (6)	Particle Froude number, $F_d = U_o/\sqrt{gD_{50}}$ (7)	Critical particle Froude number, $F_{dc} = U_c/\sqrt{gD_{50}}$ (8)
F-1	0.25	10.2	0.50	0.50	0.29	10.10	5.86
F-2	0.25	10.2	0.75	0.75	0.29	15.24	5.86
F-3	0.25	10.2	1.00	1.00	0.29	20.19	5.86
F-4	0.25	10.2	1.20	1.20	0.29	24.23	5.86
M-1	1.50	10.2	0.50	0.50	0.50	4.12	4.12
M-2	1.50	10.2	0.65	0.65	0.50	5.36	4.12
M-3	1.50	10.2	0.75	0.75	0.50	6.18	4.12
M-4	1.50	10.2	0.85	0.85	0.50	7.01	4.12
M-5	1.50	10.2	1.00	1.00	0.50	8.24	4.12
M-6	1.50	10.2	1.20	1.20	0.50	9.89	4.12
M-7	1.50	10.2	1.50	1.50	0.50	12.37	4.12
C-1	2.50	10.2	0.50	0.50	0.63	3.19	4.02
C-2	2.50	10.2	0.62	0.62	0.63	3.96	4.02
C-3	2.50	10.2	0.75	0.75	0.63	4.79	4.02
C-4	2.50	10.2	1.00	1.00	0.63	6.39	4.02
C-5	2.50	10.2	1.20	1.20	0.63	7.66	4.02
C-6	2.50	24.7	0.82	0.53	0.46	5.24	4.57
C-7	2.50	21.6	1.41	0.96	0.48	9.00	4.46
C-8	2.50	24.1	0.79	0.51	0.47	5.04	4.61

[a]Unless indicated otherwise.

scour was devised. The method involved embedding strings of yarn vertically in the sand, in a square grid pattern around each pier. As the bed eroded, the strings were bent over at the bed and when the bed aggraded, the strings were covered over, preserving the lowest level of scour (see Fig. 3). Upon completion of each run, the strings were carefully excavated and the scour depth measured with the point gage. Figs. 4(*a*) and 4(*b*) are two photographs depicting the grid pattern and excavation work. The overall grid size was 48.8 cm × 73.2 cm, and the rows and columns were spaced at 6.1 cm intervals.

The maximum scour value for each run was the difference between the MBE and the measured scour. Also, since some of the upstream strings in the grid pattern were beyond the influence of the pier, it was possible to determine local bed degradation below the MBE, due to migrating bed forms.

Depth Tests.—For the depth tests, the channel width was reduced to 61 cm by means of a temporary partition, and a third pump with a 15-cm return line installed to increase the discharge to 184 L/s. The additional pump withdrew water from the downstream end of the flume and discharged it back upstream

Parameters and Model Results

Slope, $S \times 10^{-4}$ (9)	Maximum scour due to bedforms, in centimeters (10)	MAXIMUM TOTAL SCOUR d_s, in centimeters: b = 5.08 cm (y_o/b = 2)[a] (11)	MAXIMUM TOTAL SCOUR d_s, in centimeters: b = 10.16 cm (y_o/b = 1) (12)	d_s/b: b = 5.08 cm (y_o/b = 2) (13)	d_s/b: b = 10.16 cm (y_o/b = 1) (14)	Bed condition (15)
20	0.9	8.4	12.0	1.65	1.18	Dunes
22	0.3	9.9	15.0	1.95	1.48	Flat
39	2.1	11.4	15.9	2.24	1.56	Antidunes
63	3.4	15.7	18.5	3.09	1.82	Chutes and pools
12	0	8.6	13.2	1.69	1.30	Incipient motion
35	2.7	8.7	12.3	1.71	1.21	Dunes
51	3.0	8.6	12.4	1.69	1.22	Dunes
73	4.9	9.8	13.9	1.93	1.37	Dunes
112	6.7	11.5	15.4	2.26	1.52	Antidunes
137	6.7	12.9	17.4	2.54	1.71	Antidunes
160	6.4	15.0	—	2.95	—	Chutes and pools
13	0	9.7	16.0	1.91	1.57	Flat
19	0	7.3	14.1	1.44	1.39	Incipient motion
40	2.4	7.5	13.9	1.48	1.37	Dunes
113	3.4	10.3	14.9	2.03	1.47	Dunes
169	5.8	10.7	15.9	2.11	1.56	Dunes
10	1.8	8.7 (y/b = 4.9)	—	1.71 (y/b = 4.9)	—	Dunes
65	5.2	11.3 (y/b = 4.3)	—	2.22 (y/b = 4.3)	—	Dunes
10	1.8	9.4 (y/b = 4.7)	—	1.85 (y/b = 4.7)	—	Dunes

into the flume through a diffuser box. Only the 5.08-cm pier was used in these tests because of the excessive blockage produced by the larger pier. The approximate flow depth for the depth tests was 22 cm. The procedures for establishing uniform flow and measuring scour were the same as before.

As a check on width effects, a run was made without the partition (Run No. C-8 in Table 2), and the scour depth was compared to that obtained from a similar run, made with the partition (Run No. C-6). The scour depths were nearly identical, and it was concluded that width effects were negligible.

Experimental Results

Test Parameters.—The flow conditions for the various runs and the principal results obtained in these tests are summarized in Table 2. The critical velocity, V_c, used in computing the critical Froude number given in Col. 6 of Table 2, is based on the logarithmic velocity distribution [$V_c/V_* = 2.5 \ln (11.02 y_o x/D_{50})$, in which V_* = critical shear velocity; and x = a correction factor

accounting for the effect of viscosity], and the Shield's criterion for the critical shear stress (12). The maximum scour below the mean bed elevation due to bed-forms only, listed in Col. 10, is the average of the scour readings measured

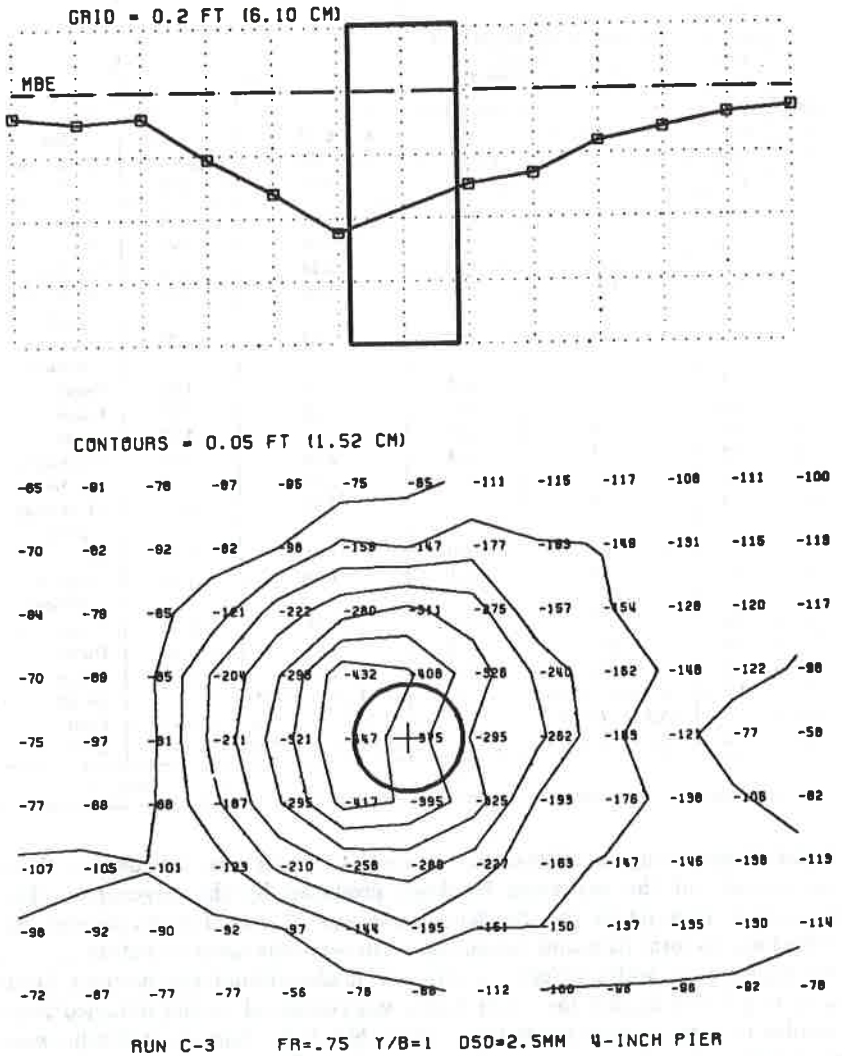

Longitudinal cross section and contours of the scour hole. Run C-3

FIG. 5.—Center Line Profile and Contour Plots of Scour from Typical Run

at the embedded strings located 6 pier diameters (the most upstream row), upstream of the smaller pier. The examination of the longitudinal cross sections of the scour holes showed that the scour hole around the pier did not affect

the scour due to bed-forms this far upstream of the pier. The scour depths presented in Cols. 11 and 12 are the maximum values below the mean bed elevation observed near the upstream end of the piers, and include the effect of bed-forms. Runs No. C-6 and C-7 were conducted with a reduced flume width of 61 cm. The flows at Froude number 1.2 and higher in the flume were very rough. The flow conditions for Runs F-4 and M-7 in particular, were unstable, and the results for these runs are, therefore, questionable. The bed-form conditions for the various runs are given in Col. 15. No flat-bed regime was observed in the tests with the medium and coarse sands.

Shape of the Scour Hole.—The data on measured scour depths around each pier were punched on cards; the longitudinal cross section through the center of the pier, and the contours of the scour hole were plotted by computer. A typical plot for Run C-3 is shown in Fig. 5. The numbers in the contour plot of Fig. 5 indicate scour depth in thousandths of a foot below the mean bed elevation. The scour holes were similar to a frustum of an inverted cone, and the maximum scour depth always occurred at the upstream end of the pier. Similar observations were recorded by earlier investigators (3,11).

Dimensional Analysis.—Depth of scour, d_s, is the dependent variable in this study. It can be expressed as a function of the other independent variables:

$$d_s = f(\phi, b, l, y_o, U_o, \rho, \nu, D_{50}, \sigma_g, \rho_s, g, t) \quad \ldots \ldots \ldots \ldots \ldots \ldots \ldots \ldots \quad (1)$$

in which ϕ = pier shape factor; b = pier width perpendicular to the approach flow; l = pier length parallel to the approach flow; y_o = depth of approach flow; U_o = velocity of approach flow; ρ = fluid density; ν = fluid kinematic viscosity; D_{50} = mean sediment diameter; σ_g = geometric distribution of sediment diameters about the mean; ρ_s = sediment density; g = gravitational acceleration; and t = time. It can be argued (9), that ρ_s of itself is not as significant as is its submerged weight, $\gamma_s' = g(\rho_s - \rho)$, which gives a measure of the buoyancy forces acting on a particle. Substituting γ_s' for ρ_s, Eq. 1 can be nondimensionalized as

$$\frac{d_s}{b} = f\left(\phi, \frac{l}{b}, \frac{y_o}{b}, \frac{U_o b}{\nu}, \frac{D_{50}}{y_o}, \sigma_g, \frac{\rho U_o^2}{\gamma_s' D_{50}}, \frac{U_o}{\sqrt{g y_o}}, \frac{U_o t}{b}\right) \quad \ldots \ldots \ldots \ldots \quad (2)$$

in which $\rho U_o^2/\gamma_s' D_{50}$ = a variation of Shield's parameter for the beginning of bed movement, with the shear velocity replaced by the mean stream velocity. Some of the terms in Eq. 2 can be eliminated. The variables ϕ and l/b, are constants in this study, because the piers are circular. The effect of viscosity is considered negligible in the scour process so that $U_o b/\nu$ can be dropped. The value, σ_g, is approximately constant for the three sands with values ranging only from 1.25–1.34. And $U_o t/b$ is not relevant, since time development of scour was not of interest in this study. Thus, Eq. 2 can be reduced to

$$\frac{d_s}{b} = f\left(\frac{y_o}{b}, \frac{D_{50}}{y_o}, \frac{\rho U_o^2}{\gamma_s' D_{50}}, \frac{U_o}{\sqrt{g y_o}}\right) \quad \ldots \ldots \ldots \ldots \ldots \ldots \ldots \ldots \quad (3)$$

The particular form of $U_o/\sqrt{gy}$ = F, the Froude number of the approach flow, is chosen because of the possible effects of surface waves on scour at high flow velocities. If further analysis is limited to sand in water, then ρ and $\rho_s - \rho$ are constants and the term, $\rho U_o^2/\gamma_s' D_{50}$, is in effect a Froude number

in which D_{50} = the characteristic length: $F_d = U_o/\sqrt{gD_{50}}$. Hereinafter, F_d is referred to as the particle Froude number. For a given flow velocity, flow depth, and particle size, F and F_d differ only by a constant, indicating that one of the terms is redundant. Furthermore, the relative sediment size, D_{50}/y_o, can be expressed as a function of $F_c = U_c/\sqrt{gy_o}$ or $F_{dc} = U_c/\sqrt{gD_{50}}$, using Shield's criterion for the initiation of sediment movement and the logarithmic velocity distribution, in which U_c = critical velocity for the initiation of sediment

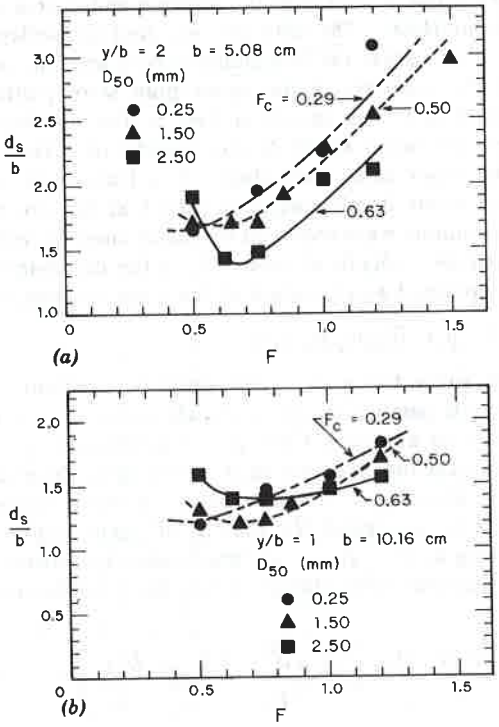

FIG. 6.—Scour Depth Versus Froude Number Plots of Experimental Data

movement. Thus, Eq. 3 can be written either as

$$\frac{d_s}{b} = f\left(\frac{y_o}{b}, F_c, F\right) \quad \ldots\ldots\ldots\ldots\ldots\ldots\ldots\ldots\ldots\ldots\ldots\ldots\ldots\ldots\ldots\ldots (4a)$$

$$\text{or} \quad \frac{d_s}{b} = f\left(\frac{y_o}{b}, F_{dc}, F_d\right) \quad \ldots\ldots\ldots\ldots\ldots\ldots\ldots\ldots\ldots\ldots\ldots\ldots\ldots\ldots\ldots\ldots (4b)$$

Data Analysis.—In light of the dimensional analysis and the choice of the Froude number as an independent variable, the variations of relative scour depth are plotted in Figs. 6 and 7. The plots in Fig. 6 are based on the Froude number, F, and the plots in Fig. 7 are based on the particle Froude number, F_d. The critical Froude number and the critical particle Froude number for

incipient sediment motion, F_c and F_{dc}, respectively, are indicated for each of the sand sizes. The scour depth first decreases and then increases, with an increasing Froude number (or velocity). This can be explained in the following way. Maximum clear water scour is that condition in which the scour mechanism can no longer dislodge particles near the base of the pier when the stream is flowing at incipient sediment motion conditions. If the stream velocity is increased, then the strength of the scour mechanism increases, but now sediment is also transported into the scour hole. If the sediment transport rate into the hole is greater than the corresponding increase in sediment removal rate by

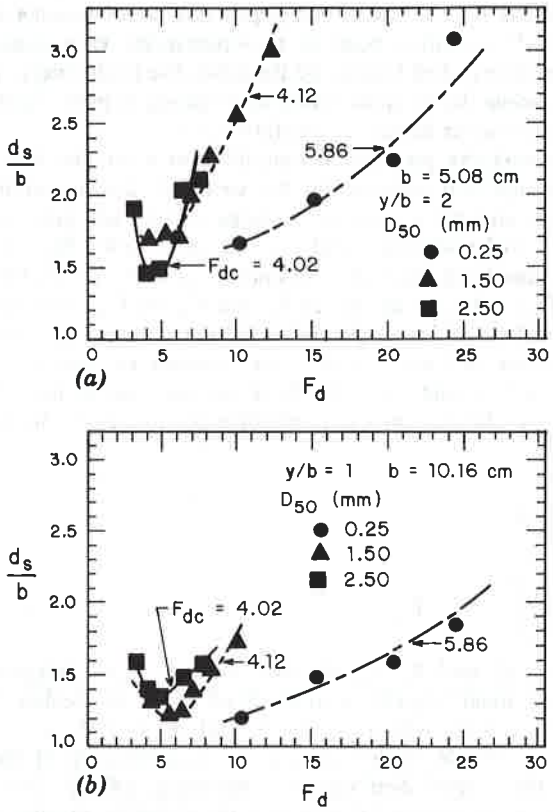

FIG. 7.—Scour Depth Versus Particle Froude Number Plots of Experimental Data

the scour mechanism, then the net result is a decrease in scour depth, whereupon the new maximum scour depth is marked by the equilibrium between sediment transport rate into the hole and the sediment removal rate by the scour mechanism. As the stream velocity is further increased, the strength of the scour mechanism continues to increase, as does the sediment transport rate. However, the scour mechanism strength increases more quickly with the result that the equilibrium between sediment transport rate into the scour hole and sediment removal rate by the scour mechanism is characterized by a greater scour depth. This reduction

in the scour depth at velocities slightly higher than the critical velocity was reported by previous investigators. The increase in the scour depth with Froude number (or velocity) for $(F - F_c) > 0.15$ is, however, not in accord with their conclusion. The reason for this discrepancy possibly lies in the scour measuring techniques.

A comparison of the total scour depth (Cols. 11 and 12 of Table 2), to the maximum scour due to bed-forms alone (Col. 10), shows that the contribution of the latter to the former in most cases becomes significant as the velocity increases. However, it should not be concluded that the increase in the scour depth is primarily due to bed-forms; the total scour depth in Run F-2 is higher than that in Run F-1, but the scour depth due to bed-forms alone has the opposite trends. It is neither possible to separate the two components of the scour depth (one due to bed-forms and the other due to the pier), nor necessary, since the total scour depth is required in designing a pier. Thus, the formula to predict the total scour depth will be developed.

The scour around the pier reaches equilibrium when the time average rate of sediment erosion and removal by the vertically downward flow along the face of the pier, and the system of vortices around the pier, is equal to the time average rate of sediment supply to the scour hole. The latter, according to Onishi, Jain, and Kennedy (10), is proportional to $(F - F_c)^n$. This observation suggests that F and F_c in Eq. 4*a* or F_d and F_{dc} in Eq. 4(*b*) can be grouped as $(F - F_c)$ or $(F_d - F_{dc})$, respectively. If the data points corresponding to each of the curves in Figs. 6 and 7 are selected so that: (1) The value of $F > F_c$ or $F_d > F_{dc}$; and (2) only those consecutive points which increase monotonically are chosen, then it is possible to fit a curve to the data of the form

$$\frac{d_s}{b} = A_1 \left(\frac{y_o}{b}\right)^{\alpha_1} (F - F_c)^{\beta_1} \quad \ldots\ldots\ldots\ldots\ldots\ldots\ldots\ldots\ldots\ldots\ldots\ldots\ldots\ldots (5a)$$

$$\text{or} \quad \frac{d_s}{b} = A_2 \left(\frac{y_o}{b}\right)^{\alpha_2} (F_d - F_{dc})^{\beta_2} \quad \ldots\ldots\ldots\ldots\ldots\ldots\ldots\ldots\ldots\ldots\ldots\ldots\ldots\ldots (5b)$$

in which A_1, α_1, β_1 and A_2, α_2, β_2 are constants to be determined from the data. A multiple-linear regression analysis of the data yielded $A_1 = 1.86$; $\alpha_1 = 0.49$; and $\beta_1 = 0.26$, with $r^2 = 0.896$; and $A_2 = 1.19$; $\alpha_2 = 0.52$; and $\beta_2 = 0.14$, with $r^2 = 0.746$. (The variable, r^2, is a measure of the dependence of d_s/b upon the independent variables operating jointly. The value $r^2 = 1$ indicates a perfect correlation.) Based upon the r^2 values, the regression analysis shows that Eq. 5*a* is the preferred form of the functional relationship, since Eq. 5*a* yields a better fit to the data. By rounding values of α_1 and β_1 to the nearest 1/4, and substituting them and the value for A_1 into Eq. 5*a*, the following predictor equation is obtained:

$$\frac{d_s}{b} = 1.86 \left(\frac{y_o}{b}\right)^{0.5} (F - F_c)^{0.25} \quad \ldots\ldots\ldots\ldots\ldots\ldots\ldots\ldots\ldots\ldots\ldots\ldots\ldots\ldots (6)$$

Fig. 7 shows that all of the curves increase monotonically if $F - F_c \geqq 0.15$. A plot of the data using Eq. 6 with the restrictions $0.15 \leq (F - F_c) \leq [1.2]$ and $[1] \leq y/b \leq 2$ is given in Fig. 8, with additional data included from

studies by Chabert and Engeldinger (3), and Shen, et al. (11), for comparative purposes. Some of their data points, particularly for which the flow velocity was much higher than the threshold velocity, lie below the regression line. This discrepancy is probably due to the scour measuring technique they used. Shen, et al. stopped the flow before measuring scour depths. Chabert and Engeldinger, in their report, did not specify whether scour measurements were taken after the flow closure or under running flow conditions. If the latter is true, it is extremely difficult to accurately locate the bottom of the scour hole with the ruler used to measure the scour depth. Eq. 5*a* with $A = 2.0$, envelopes all the data for $(F - F_c) \geq 0.2$ except for two data points corresponding to Runs F-4 and M-7, in which flow conditions in the flume were unsteady due to the formation of chutes and pools on the bed.

Depth Tests.—To evaluate the effects on scour of very large relative depths, a few tests (Runs No. C-6, C-7, and C-8), using only the smaller pier, were

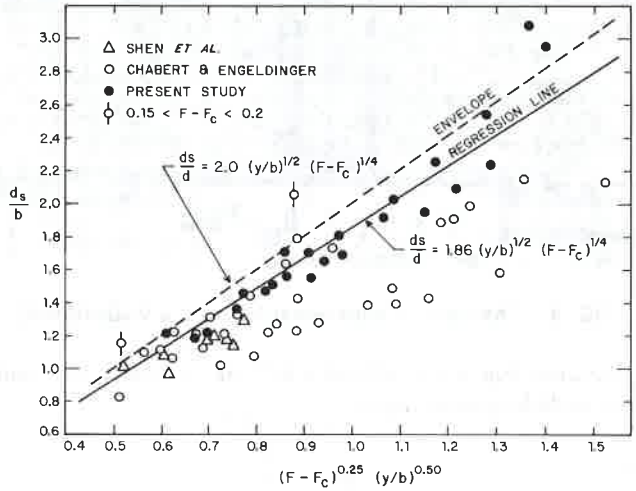

FIG. 8.—Comparison of Eq. 6 to Experimental Data

conducted at relative depths of about 5. The flow conditions for Runs C-6 and C-8 were almost identical, except the flume widths in the two runs were 61 cm and 91 cm, respectively. The data for Run C-7 were not used in the correlation analysis, because this was the only data point available on scour depth at high Froude number and relative depth. The observed scour for run C-7 was about 70% of the scour predicted by Eq. 5*a* with $A = 1.86$, indicating that Eq. 5*a*, which was developed using data only for $y/b = 1$ and 2, overpredicts scour depths at high relative depths.

Flow Visualization.—It was instructive to watch the scour process around the half-piers placed against the flume wall, as shown in Fig. 9. The grid spacing was 3.05 cm, and the arrows indicate the approximate MBE. The flow was from left to right. One could see the sediment transported into the scour hole, the scour mechanism at the base of the pier, and the sediment being carried from the scour hole. The visual observation indicated that the scour depth

fluctuated with time, but not always in phase with passing dunes. The visualization also demonstrated that a dynamic equilibrium exists between scour hole and streamflow which is not apparent when the flow is stopped; the flow field near the base of the pier is strong enough to support the sides of the scour hole at angles greater than the angle of repose of the sediment. In fact, the scour hole can, at times, be nearly vertical. The wall periodically collapsed and dumped sediment into the hole, either as a dune encroached upon the pier or as the fluid forces supporting it became unstable. In similar tests, Shen,

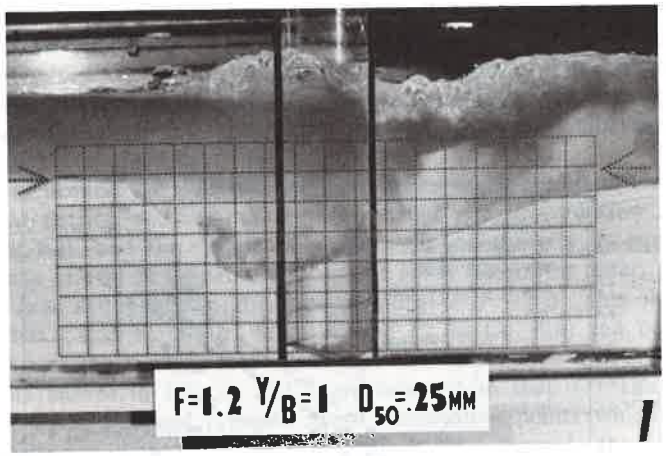

FIG. 9.—Photograph Representative of Flow Visualization

et al. (11), reported that scour around a half-pier is nearly the same as scour around a pier, including scour depth.

Conclusions

Experimental results from this study show that after decreasing slightly, upon the onset of sediment transport in a stream, scour depth does increase again with increasing velocity. A special technique was employed to measure scour depths. A predictor for scour depth at high flow velocities in the sediment transport regime was developed from the data and is given by Eq. 6.

Acknowledgment

This study was sponsored by the United States Department of Transportation under contract number DOT-FH-11-9276.

Appendix I.—References

1. Anderson, A. G., "Scour at Bridge Waterways—A Review," *Report No. FHWA-RD-75-89,* Federal Highway Administration, Washington, D.C., 1974.
2. Breusers, H. N. C., Nicollet, G., and Shen, H. W., "Local Scour Around Cylindrical Piers," *Journal of Hydraulic Research,* International Association for Hydraulic Research, Vol. 15, No. 3, 1977.
3. Chabert, J., and Engeldinger, P., "Etude des Affouillements Autour des Piles des Ponts," Laboratoire National d'Hydraulique, Chatou, France, 1956.
4. Jain, S. C., and Fischer, E., "Scour Around Bridge Piers at High Froude Numbers," *Report No. FH-WA-RD-79-104,* Federal Highway Administration, Washington, D.C., Apr., 1979.
5. Hinze, J. O., *Turbulence,* McGraw-Hill Publishing Co., Inc., New York, N.Y., 1959.
6. Melville, B. W., "Local Scour at Bridge Sites," *Report No. 117,* University of Auckland, School of Engineering, Auckland, New Zealand, 1975.
7. Miller, J. P., and Leopold, L. B., "Simple Measurements of Morphological Changes in River Channels and Hill Slopes," Changes of Climate, *Proceedings of the Rome Symposium organized by United Nations Educational, Scientific, and Cultural Organization and the World Meteorological Organization,* 1963.
8. Neill, C. R., "Local Scour Around Bridge Piers," Highway and River Engineering Division, Research Council of Alberta, Alberta, Canada, 1964.
9. Neill, C. R., discussion of "Local Scour Around Bridge Piers," by Shen, H. W., Schneider, V. R., and Karak, S., *Journal of the Hydraulics Division,* ASCE, Vol. 96, No. HY5, Proc. Paper 6891, May, 1970, pp. 1224–1227.
10. Onishi, Y., Jain, S. C., and Kennedy, J. F., "Effects of Meandering in Alluvial Streams," *Journal of the Hydraulics Division,* ASCE, Vol. 102, No. HY7, Proc. Paper 12248, July, 1976, pp. 899–917.
11. Shen, H. W., Schneider, V. R., and Karaki, S., "Mechanics of Local Scour," *Report No. CER 66 HWS-SK22,* Colorado State University, Fort Collins, Colo., 1966.
12. Vanoni, V. A., ed., *Sedimentation Engineering,* Manuals and Reports on Engineering Practice, No. 54, ASCE, 1975.
13. Vanoni, V. A., et al., "Lecture Notes on Sediment Transportation and Channel Stability," *Report No. KH-R1,* W. M. Keck Laboratory of Hydraulics and Water Resources, California Institute of Technology, Pasadena, Calif., 1961.

Appendix II.—Notation

The following symbols are used in this paper:

A_1, A_2 = empirically determined coefficients;
b = horizontal pier width;
d_s = scour depth below mean bed elevation;
d_{sc} = clear water scour depth below mean bed elevation;
D_{50} = mean sediment size;
F = Froude number;
F_c = critical Froude number for incipient sediment motion;
F_d = particle Froude number;
F_{dc} = critical particle Froude number for incipient sediment motion;
g = acceleration due to gravity;
l = horizontal pier length;
r = statistical correlation coefficient;
t = time;
U_c = average critical velocity for initiation of sediment motion;
U_o = average approach flow velocity;
y_o = average depth of approach flow;
$\alpha_1, \alpha_2, \beta_1, \beta_2$ = empirically determined exponents;
γ_s' = submerged specific weight of sediment;
ν = ambient fluid kinematic viscosity;
ρ = ambient fluid density;

ρ_s = sediment density;
σ_g = geometric distribution of sediment size about mean; and
ϕ = pier shape.

JOURNAL OF THE HYDRAULICS DIVISION

Modeling Three-Dimensional Wind-Induced Flows

By Christopher Koutitas,[1] M. ASCE and Brian O'Connor[2]

Introduction

The impact of new engineering works on the coastal environment has traditionally been examined by means of field measurements (13,18), supplemented by laboratory studies, involving small-scale hydraulic models (2,7,16). In recent years, however, advances in computer technology have enabled engineers to replace some of the field and laboratory work by computer calculations (1,11,12, 19), which often involve complex ideas on the simulation of frictional energy losses (10,17). Unfortunately, the more complex computational procedures (or mathematical models, as they are called), require the use of very powerful computers; consequently, attempts have been made to produce simpler models, which are still capable of studying complex three-dimensional flows (4,5,8). It also appears that the use of highly complex energy loss equations may be unnecessary, since modeling of estuary flows (17), shows that such techniques do not lead to a significant improvement in the accuracy of engineering calculations.

The present study thus examines the computer modeling of three-dimensional coastal flows with the object of producing a new relatively simple model, which overcomes the problems of earlier models (4), and which will also be more generally applicable. The study also examines the methods used to simulate energy losses in earlier models (10,11,17,19), and uses computations and laboratory tests in order to choose the most appropriate method to incorporate in the new model.

Note.—Discussion open until April 1, 1981. To extend the closing date one month, a written request must be filed with the Manager of Technical and Professional Publications, ASCE. This paper is part of the copyrighted Journal of the Hydraulics Division, Proceedings of the American Society of Civil Engineers, Vol. 106, No. HY11, November, 1980. Manuscript was submitted for review for possible publication on September 24, 1979.

[1]Prof. of Coast and Harbor Engrg., Demokritos Univ., Xanthi, Greece.
[2]Sr. Lect., Dept. of Engrg., Simon Engrg. Labs., Univ. of Manchester, Manchester, England.